

Representing the cortex convolutions through the wrinkling of growing soft bilayers

Martine Ben Amar and Adrien Bordner

Laboratoire de Physique de l'ENS
& Institut de Cancérologie de Sorbonne Université
Conférence Neobrain

9 Mars 2021, Paris

Recent interest for brain embryology, why?

- New techniques in vivo, like MRI
- Cerebrum sulci = cognition support
- Development, pathologies of development

Recent interest for brain embryology, why ?

- New techniques in vivo, like **MRI**
- Cerebrum sulci = cognition support
- Development, pathologies of development

New techniques and new possibilities for investigation

- Progress and challenges in probing the human brain, Nature (2015)
- A multi-modal parcellation of human cerebral cortex, M. Glasser et al. Nature (August,2016) and The human connectome project's neuroimaging approach, Nat. Neurosciences (in press)

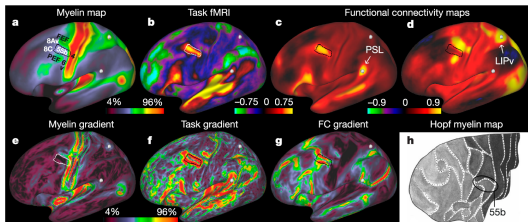


Figure – A HCP parcellation, 180 areas per hemisphere

Theory of elasticity : Volumetric Growth of a bilayer

- Nonlinear elasticity of tissues. Variational formalism
- Differential growth between the two layers : **grey matter and white matter**
- Special focus on wavelength selection : a challenging and controversial problem, **Biot (57), Biot (63)**
- Scope : **The gyrification index**

Adult brain anatomy



A



B

Figure – A. Section of human brain. **B.** 3D reconstruction of human brain, modelled as a soft elastic solid with growth in the cortex, Tallinen et al. , Nature Physics,2016

The central nervous system

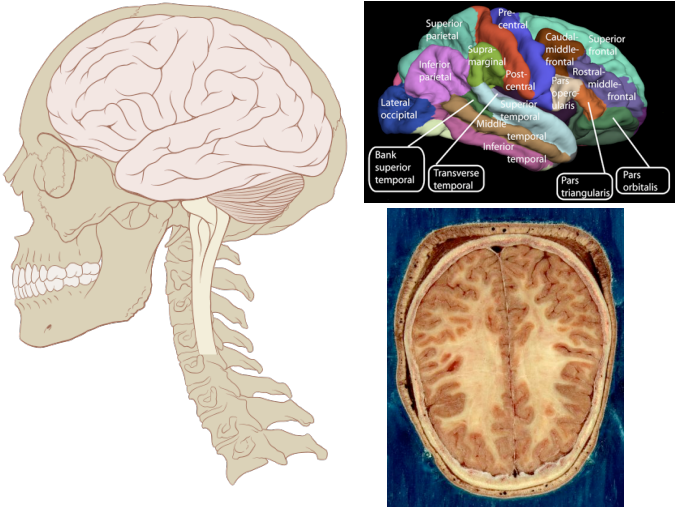


Figure – A Brain and spinal cord,B nomenclature,C cut of the brain

The brain anatomy

Two layers in the adult brain :

- The grey matter (soft)
- The white matter (stiffer, according Budday et al,2014)

The brain anatomy

Two layers in the adult brain :

- The grey matter (soft)
- The white matter (stiffer, according Budday et al,2014)

But also,

- The meninges : 3 layers
- The cerebrospinal fluid

Central Nervous System and the Cerebrum Development

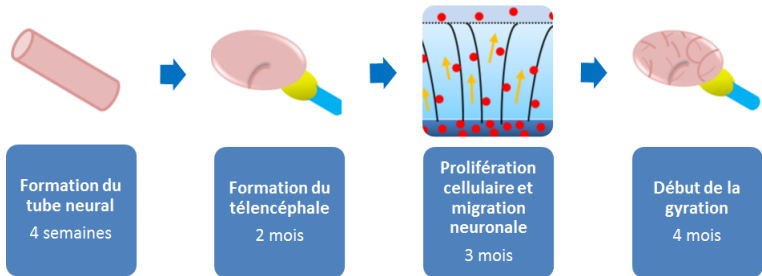


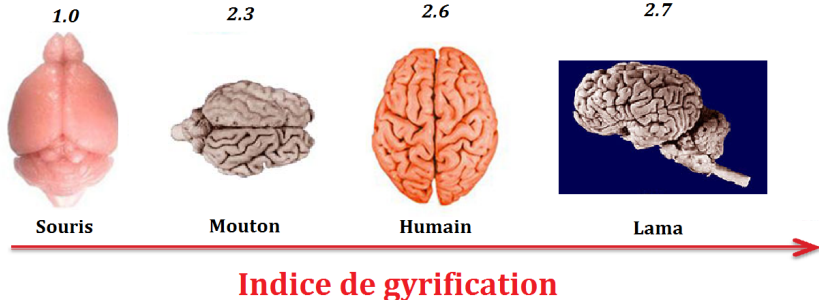
Figure – Main steps of formation as a function of Gestational Age GA

Apparition of the bilayer **before the cerebrum sulci!**

⇒ **Bilayer model** : grey matter with **neuronal bodies**, white matter : **glial cells and axons**

How to quantify the gyrification

$$\text{Index of gyrification} : G_I = \frac{\text{Full cerebrum area}}{\text{Apparent external area}}$$



Pathologies associated with gyrification

Examples

- The lissencephaly (smooth brain)
- The polymicrogyria (excessive number of small gyri)
- Local anomalies like autism, schizophrenia.....

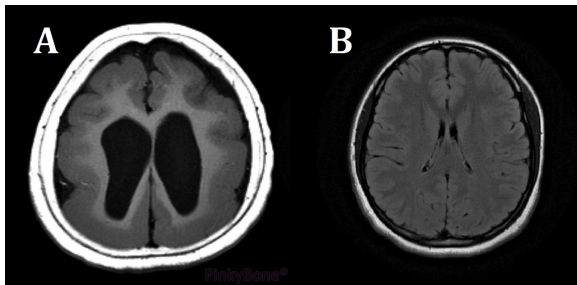


Figure – Comparison of lissencephalic (A) and healthy brain (B) by MRI

Examples of recent MRI studies

- *Simplified gyral pattern in severe developmental microcephalies? New insights from allometric modeling for spatial and spectral analysis of gyrification* D. Germanaud et al., Neuromage, (2014)
- *Are Developmental Trajectories of Cortical Folding Comparable Between Cross-sectional Datasets of Fetuses and Preterm Newborns?* J. Lefebvre, D. Germanaud...François Rousseau Cortex (2016).
- *Localized misfolding within Broca area as a distinctive feature of autistic disorder. Biological Psychiatry : Cognitive Neuroscience and Neuroimaging* , J. Brun et al. (2015).
- *A Longitudinal Study of Local Gyrification Index in Young Boys With Autism Spectrum Disorder*, L. E Libero, M. Schaer, D. D Li, D.G. Amaral & C. Wu Nordahl (Cereb Cortex 2018)

Models

Two kinds of models :

Models for gyri formation

- **Mechanical models**, like " axonal tension " (Manyuhina 2014) \Rightarrow more or less pre-strain, pre-stress models
- **Differential growth.**
- **Numerical** (R. Toro and Y. Burnod, 2005, Tallinen *et al.* 2014)
- **Theoretical** : 2 layers with 2 different thicknesses, volumetric differential growth,

\Rightarrow 2 famous papers of Biot, Biot (57) and Biot (63)

Proceedings of the Royal Society, A, volume 242, pp. 444-454, 1957

Folding instability of a layered viscoelastic medium under compression

By M. A. BIOT

Shell Development Company

(Communicated by Sir Geoffrey Taylor, F.R.S.—Received 6 April 1957)

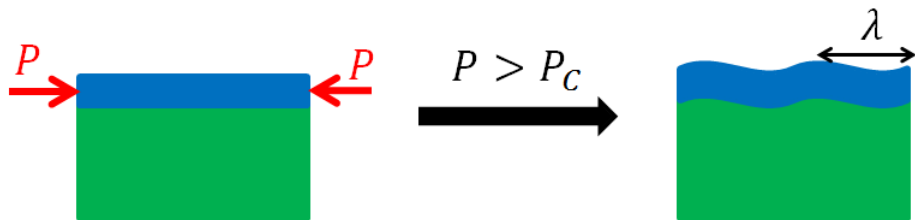
SURFACE INSTABILITY OF RUBBER IN COMPRESSION

by M. A. BIOT

New York, U.S.A.

One or two layers under compression

Biot (57) One thin, stiff layer on an infinite soft substrate

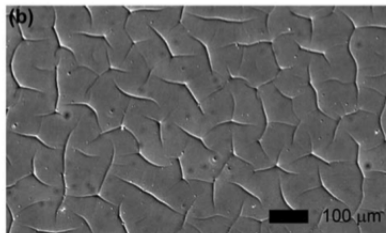
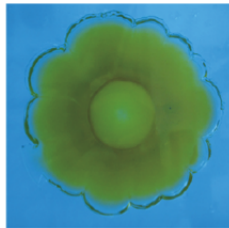
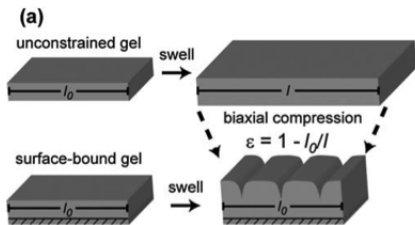


- $\mu = \frac{\mu_1}{\mu_2}$ with $\mu \rightarrow \infty$
- A critical threshold $P_c \sim \mu^{-1/3}$
- A wavelength $\lambda_c \sim \mu^{1/3}$.

Origin : Long wavelength limit $\lambda \gg H$. **The human brain** is not concerned by this limit : $\mu \sim 0.7$ (like bovine, pigs)

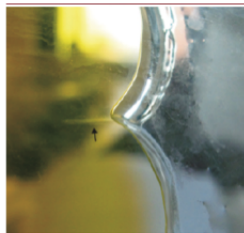
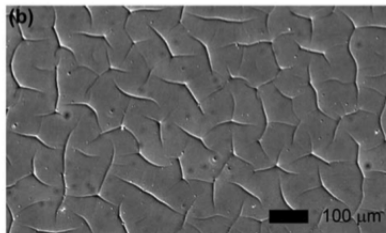
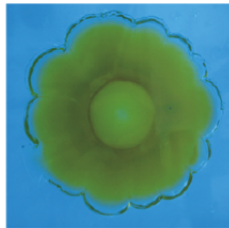
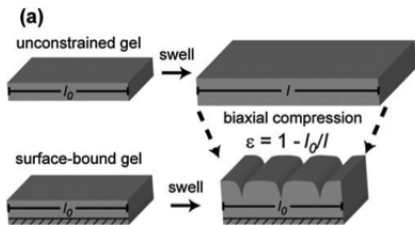
Biot's singularity or surface instability

Biot' singularity (63) one Neo-Hookean infinite layer, a finite threshold but $\lambda \rightarrow 0$ so **creases**!!!!!!



Biot's singularity or surface instability

Biot' singularity (63) one Neo-Hookean infinite layer, a finite threshold but $\lambda \rightarrow 0$ so **creases**!!!!!!



Method

Main physical ingredients

- Ratio of stiffnesses $\mu = \frac{\mu_G}{\mu_W} \sim 0.7$
- **Anisotropic growth** in the cortex (more **proliferation** at the interface cortex/white matter, no **known** order of magnitude)
- Differential growth : **Growth which is different in grey and white matter**
- Infinite (or not) substrate ($L_W \gg L_G$)

Method

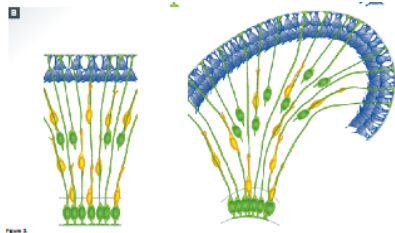
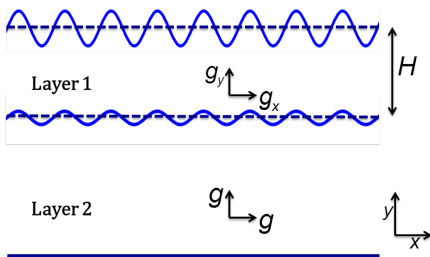
Main physical ingredients

- Ratio of stiffnesses $\mu = \frac{\mu_G}{\mu_W} \sim 0.7$
- **Anisotropic growth** in the cortex (more **proliferation** at the interface cortex/white matter, no **known** order of magnitude)
- Differential growth : **Growth which is different in grey and white matter**
- Infinite (or not) substrate ($L_W \gg L_G$)

Questions

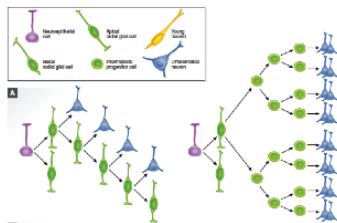
- 1) Instability threshold ?
- 2) Biot's singularity ? Can we get a finite wavelength ?
- 3) Post-buckling analysis an Gyrification index ?
- 4) Can we go back to pathologies ?

Elastic bilayer



Scheme of the model. Cortex growth from « cortex growth expansion...Fernandez et al. EMBO (2016)

$(X,Y) \rightarrow (x,y)$



Multiplicative decomposition gradient

Geometric deformation gradient : $\mathbf{F} = \begin{bmatrix} \frac{\partial x}{\partial X} & \frac{\partial x}{\partial Y} \\ \frac{\partial y}{\partial X} & \frac{\partial y}{\partial Y} \end{bmatrix}$

First hypothesis, [Rodriguez 1994]

If we have a separation of time scales, if growth is very slow, $\mathbf{F} = \mathbf{F}_e \cdot \mathbf{G}$:

- Elastic tensor : \mathbf{F}_e
- Growth tensor : $\mathbf{G}_1 = \begin{bmatrix} g_x & 0 \\ 0 & g_y \end{bmatrix}$ and $\mathbf{G}_2 = \begin{bmatrix} g & 0 \\ 0 & g \end{bmatrix}$

Multiplicative decomposition gradient

Geometric deformation gradient : $\mathbf{F} = \begin{bmatrix} \frac{\partial x}{\partial X} & \frac{\partial x}{\partial Y} \\ \frac{\partial y}{\partial X} & \frac{\partial y}{\partial Y} \end{bmatrix}$

First hypothesis, [Rodriguez 1994]

If we have a separation of time scales, if growth is very slow, $\mathbf{F} = \mathbf{F}_e \cdot \mathbf{G}$:

- Elastic tensor : \mathbf{F}_e
- Growth tensor : $\mathbf{G}_1 = \begin{bmatrix} g_x & 0 \\ 0 & g_y \end{bmatrix}$ and $\mathbf{G}_2 = \begin{bmatrix} g & 0 \\ 0 & g \end{bmatrix}$

Second hypothesis

Living tissues are incompressible, so any change of volume is due to growth.

$$J_1 = g_x g_y \text{ et } J_2 = g^2$$

Incompressibility and stream functions

Definition of stream functions

Analogy with hydrodynamics, we define $\Phi(x_1, Y_1)$ et $\Psi(x_2, Y_2)$:

$$X_1 = J_1^{-1} \frac{\partial \Phi}{\partial Y_1}$$

$$y_1 = \frac{\partial \Phi}{\partial x_1}$$

$$X_2 = J_2^{-1} \frac{\partial \Psi}{\partial Y_2}$$

$$y_2 = \frac{\partial \Psi}{\partial x_2}$$

Advantage :

- We work in the correct space of deformations $\Rightarrow \emptyset$ we avoid Lagrange multiplier

Euler-Lagrange equations

Trivial growth configuration and perturbation :

$$\Phi(x, Y) = xYg_1g_2 + \varepsilon\phi(x, Y)$$

Euler-Lagrange equations

Trivial growth configuration and perturbation :

$$\Phi(x, Y) = xYg_1g_2 + \varepsilon\phi(x, Y)$$

Mode Fourier expansion :

$$\phi(x, Y) = F_1(Y)\sin(kx) \text{ and } \psi(x, Y) = F_2(Y)\sin(kx)$$

Euler-Lagrange equations

Trivial growth configuration and perturbation :

$$\Phi(x, Y) = xYg_1g_2 + \varepsilon\phi(x, Y)$$

Mode Fourier expansion :

$$\phi(x, Y) = F_1(Y)\sin(kx) \text{ and } \psi(x, Y) = F_2(Y)\sin(kx)$$

At order ε :

$$\frac{d^4 F_1(Y)}{dY^4} - k^2(J_1^2 + p^2) \frac{d^2 F_1(Y)}{dY^2} + J_1^2 p^2 k^4 F_1(Y) = 0$$

$$\frac{d^4 F_2(Y)}{dY^4} - k^2(J_2^2 + 1) \frac{d^2 F_2(Y)}{dY^2} + J_2^2 k^4 F_2(Y) = 0$$

$p = \frac{g_y}{g_x}$ is anisotropy parameter.

Solutions of Euler Lagrange

Solutions for infinite substrate :

$$F_1(Y) = \cosh(J_1 kY) + A_1 \sinh(J_1 kY) + A_2 \cosh(pkY) + A_3 \sinh(pkY)$$

$$F_2(Y) = B_1 \exp(J_2 kY) + B_2 \exp(kY)$$

$k = \frac{2\pi}{\lambda}$ wavenumber

Boundary conditions \Rightarrow **Dispersion relation** in the limit $\lambda \ll 1$

$$0 = \mathbf{P}_0(J_1) \times \mathcal{P}(\mu, J_1, J_2)$$

Solutions of Euler Lagrange

Solutions for infinite substrate :

$$F_1(Y) = \cosh(J_1 kY) + A_1 \sinh(J_1 kY) + A_2 \cosh(pkY) + A_3 \sinh(pkY)$$

$$F_2(Y) = B_1 \exp(J_2 kY) + B_2 \exp(kY)$$

$k = \frac{2\pi}{\lambda}$ wavenumber

Boundary conditions \Rightarrow Dispersion relation in the limit $\lambda \ll 1$

$$0 = \mathbf{P}_0(J_1) \times \mathcal{P}(\mu, J_1, J_2)$$

Primary bifurcation : $\mathbf{P}_0(J_1) = 0$

Secondary bifurcation : $\mathcal{P}(\mu, J_1, J_2) = 0$.

Primary Bifurcation

Primary bifurcation : $\mathbf{P}_0(J_1) = -1 - \rho J_1 - 3\rho^2 J_1^2 + (\rho J_1)^3 = 0$.

- The threshold $J_c \approx 3,38\rho$
- Does not depend on the bottom layer and also on μ . \Rightarrow The instability comes only from the top layer.
- Such solution requires a surface tension γ to derive the wavelength :

$$\lambda = 4\rho\pi H / \text{Log} \left(R_1(J_2, \mu, \rho) \times \frac{2\rho(3J_c^2 - 6J_c - 1)}{\gamma J_c(J_c + 1)} \right)$$

$$\lambda \approx 4\rho\pi H / \text{Log} \left(\frac{1.8\rho}{\gamma} \times R_1(J_2, \mu, \rho) \right)$$

Primary Bifurcation

Primary bifurcation : $\mathbf{P}_0(J_1) = -1 - \rho J_1 - 3\rho^2 J_1^2 + (\rho J_1)^3 = 0$.

- The threshold $J_c \approx 3,38\rho$
- Does not depend on the bottom layer and also on μ . \Rightarrow The instability comes only from the top layer.
- Such solution requires a surface tension γ to derive the wavelength :

$$\lambda = 4\rho\pi H / \text{Log} \left(R_1(J_2, \mu, \rho) \times \frac{2\rho(3J_c^2 - 6J_c - 1)}{\gamma J_c(J_c + 1)} \right)$$

$$\lambda \approx 4\rho\pi H / \text{Log} \left(\frac{1.8\rho}{\gamma} \times R_1(J_2, \mu, \rho) \right)$$

$\Rightarrow \lambda \sim 4\rho\pi H \Rightarrow$ **Condition** : $R_1(J_2, \mu, \rho) > 0$

Reminder : $\mu = \frac{\mu_1}{\mu_2}$ and $\rho = \frac{g_y}{g_x}$

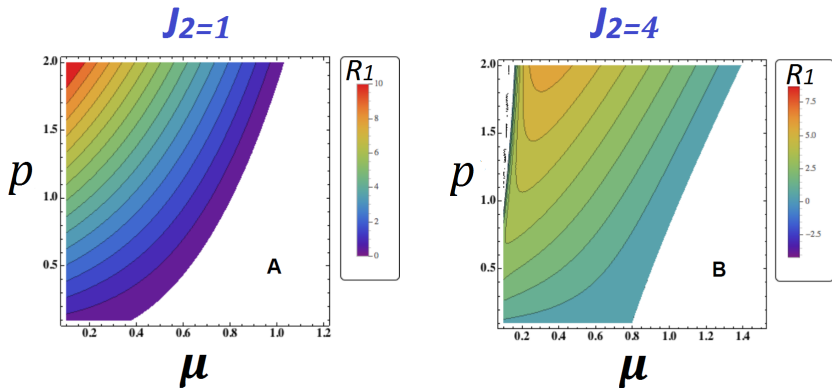


Figure – Primary bifurcation : phase diagram for R_1

Discussion

Summary

- **For a stiff substrate** ($\mu < 1$) = primary bifurcation
selection = surface tension of the upper layer
Instability originates from the upper layer
- **soft substrate** ($\mu > 1$) = secondary bifurcation
Selection = surface tension of the interface between both layers

Nano-indentation (Budday 2015) : $\mu \approx 0.6$

Conclusion

For the brain, primary bifurcation responsible of the cortical sulci. Biot Singularity : Surface Instability

Discussion : Surface tension

⇒ Not solely a mathematical tool !

The meninges

Equivalent to a surface tension or to a third layer ??? $\gamma = 4L\mu$.

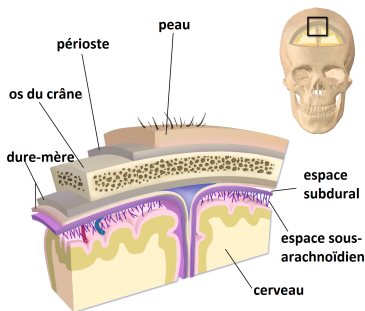


Figure – Schéma des méninges. © Blausen Medical, BruceBlaus

Discussion : pathologies

Pathologies of development = dysfunction migration of the neuronal migration \Rightarrow **modification of the growth**

Gyrification anomalies

- **Lissencephaly** (\emptyset sulci) = threshold is not reached, thick cortex.
- **Polymicrogyria** (+ tiny sulci) very weak surface tension, proliferation along the interface.
- **Local anomalies** = heterogeneity and regional variation !!

Post-buckling treatment

Up to now, no amplitude for the folds. So we need to go further and to expand the energy to next order (nonlinearities). Via **nonlinear analysis** we reach the amplitudes after post-buckling, and the nature of the bifurcation **super-critical bifurcation** :

$$\varepsilon = \pm 1.3544 \frac{e^{-HkJ_1}}{k^2} \sqrt{\rho(J_1 - J_c)} \quad (1)$$

It corresponds to MRI measurements, J. Lefebvre, D. Germanaud, F. Rousseau Cortex (2016).

Gyrification index

After the post-buckling result, we can calculate this index maintaining the "shape profile"

$$G_I = \frac{k}{2\pi} \int_{-\pi/k}^{\pi/k} \sqrt{1 + y'^2} dx = \frac{k}{2\pi} \int_{-\pi/k}^{\pi/k} \sqrt{1 + \varepsilon^2 \sin(kx)^2} dx$$

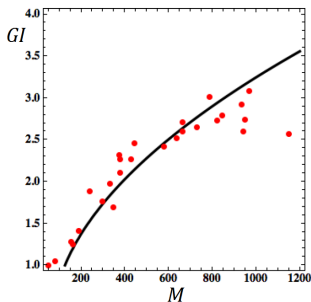


Figure – Continuous line : model ; Dots : experimental and statistical human data.
From Armstrong, E., Scleicher, A., Omran, H., Curtis, M., Zilles, K. : The ontogeny of human gyrification. *Cereb. Cortex* (1995)

Gyrification index

MRI measurements of pre-term newborns and fetuses, Lefèvre, Germanaud, F. Rousseau al.

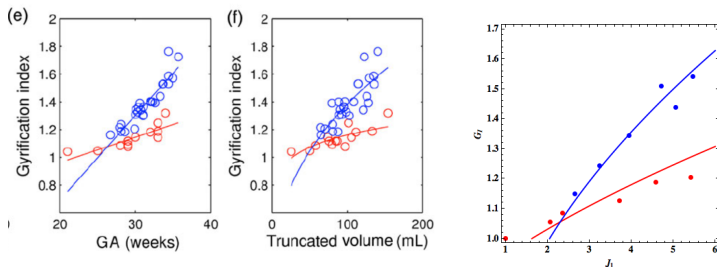
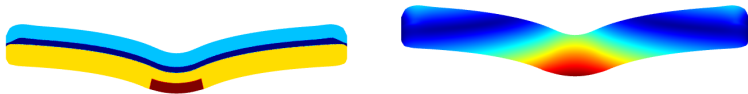


Figure – In blue pre-term newborns, in red fetuses

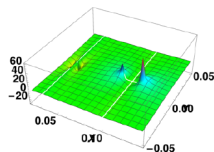
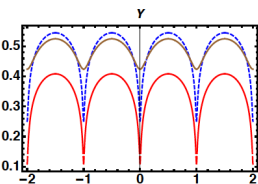
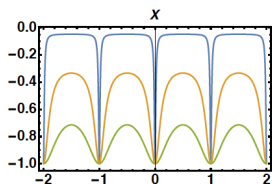
Estimation → mass of the telencephalon : 27g and 42g, anisotropy $p = .55$ and $p = 0.3$. Extrapolation far from the threshold, out of the domain of validity. Simulations are necessary.

Impact of defects or inhomogeneities

Mimicking the imaginal disk of drosophila (mutant)



Inhomogeneity of the Young modulus in an horizontal sublayer inducing a buckling. Simulations of Joseph Ackermann with COMSOL



Conclusion

- bilayer model = **not so bad**
- Very simple $J_c = 3,38\rho$ and wavelength selection $\lambda \sim 4\pi\rho H$, where H is the upper layer thickness.
- Qualitative explanation of gyri formation, G_I not a very sensitive parameter.
- Local heterogeneity
- profound sulci and creases \Leftrightarrow autism.

Other problems of bilayers in human body : skin (Ciarletta et MBA,2011) , villi (MBA and Jia, 2013), esophagus and the spinal cord ...